Automation of Spot Counting in Interphase Cytogenetics Using Brightfield Microscopy

Hans Vrolijk, Willem C.R. Sloos, Frans M. van de Rijke, Wilma E. Mesker, Hans Netten, Ian T. Young, Anton K. Raap, and Hans J. Tanke

Department of Cytochemistry and Cytometry, Medical Faculty, Leiden University, Leiden (H.V., W.C.R.S., F.M.v.d.R., W.E.M., A.K.R., H.J.T.), and Pattern Recognition Group, Faculty of Applied Physics, Delft University of Technology, Delft (H.N., I.T.Y.), The Netherlands

In situ hybridization techniques allow the enumeration of chromosomal abnormalities and form a great potential for many clinical applications. Although the use of fluorescent labels is preferable regarding sensitivity and colormultiplicity, chromogenic labels can provide an excellent alternative in relatively simple situations, e.g., where it is sufficient to use a centromere specific probe to detect abnormalities of one specific chromosome. When the frequency of chromosomal aberrations is low, several hundreds or even thousands of cells have to be evaluated to achieve sufficient statistical confidence. Since manual counting is tedious, fatiguing, and time consuming, automation can assist to process the slides more efficiently. Therefore, a system has been developed for automated spot counting using brightfield microscopy. This paper addresses both the hardware system aspects and the software image analysis algorithms for nuclei and spot detection. As a result of the automated slide analysis the system provides the frequency spot distribution of the selected cells. The automatic classification can, however, be overruled by human interaction, since each individual cell is stored in a gallery and can be relocated for visual inspection. With this system a thousand cells can be automatically analyzed in approximately 10 min, while an extra 5–10 min is necessary for visual evaluation. The performance of the system was analyzed using a model system for trisomy consisting of a mixture of male and female lymphocytes hybridized with probes for chromosomes 7 and Y. The sensitivity for trisomy detection in the seeding experiment was such that a frequency of 3% trisomic cells could be picked up automatically as being abnormal according to the multiple proportion test, while trisomy as low as 1.5% could be detected after interaction. © 1996 Wiley-Liss, Inc.

Key terms: In situ hybridization, interphase cells, brightfield microscopy, spot counting, automation, image analysis

Since the introduction of suitable alternatives for radioisotopes as markers for nucleic acid probes, in situ hybridization (ISH) has evolved as a powerful technique for biomedical research and clinical diagnosis. It allows identification and quantitation of numerical and structural chromosomal abnormalities in both metaphase spreads and interphase nuclei. Different applications have been reported such as identification of marker chromosomes (5,21); detection of translocations (4,18); detection of aneuploidy in prenatal and perinatal samples (15,25) or in various neoplasias (8,11); and study of complex chromosomal rearrangements (13,22). The ability to analyze many interphase cells forms the potential for clinical applications, such as the early detection of minimal residual disease and of relapse in leukemias and lymphomas.

Information concerning ISH can be retrieved from the number, the color, and/or the relative positions of the probe signals. Visualization of these signals can be achieved according to different approaches: first, by the use of fluoresceinated probes (direct method); second, by fluoresceinated antibodies against hapten-labeled probes (indirect method); and third, by the use of immunoenzymatic techniques (in particular, alkaline phosphatase and peroxidase) to stain the hapten-labeled nucleic acid probes. The use of fluorescent labels is preferable. Fluorescence has a higher sensitivity and allows detection of smaller target sequences than can be shown with chromogenic labels. Fluorescence also provides a simple basis for quantitation of target molecules, since theoretically for low concentrations a linear relationship between fluorescence intensity and concentration exists. In addition, multiple targets labeled with different fluorochromes can be visualized simultaneously in one preparation, since their

fluorescence emission can be well separated using proper excitation and emission filters. Under practical conditions this appears much more difficult for chromogenic labels due to the wide absorbance spectra of most dyes. On the other hand, fluorescence is a complex phenomenon, requiring careful standardization and control of many external factors.

Labels based on absorbing dyes have distinct advantages, when automation is considered. The hybridization signals are not photon limited, so that relatively cheap video-rate cameras can be applied for image acquisition and low numerical aperture (NA) lenses can be used resulting in a larger depth of focus thereby facilitating autofocusing. Another advantage of these labels is that slides can be archived for years without loss of signal or morphology. Therefore, it seems feasible to apply labels based on absorbing dyes for relatively simple cases where one probe is sufficient or where it is adequate to analyze sequentially slides stained with different probes. When centromere specific probes are used to detect aberrations of one specific chromosome in interphase nuclei such as trisomy 8 or 12 in leukemia (1,2) or trisomy 21 in Down's syndrome, labels based on absorbing dyes can provide an excellent alternative.

The manual scoring of numerical chromosomal aberrations in interphase nuclei is a tedious, fatiguing, and time-consuming job, in particular when the frequency of abnormal cells is low. Theoretical studies (6,14) have shown that several thousand interphase cells have to be evaluated in order to detect an abnormality below 5% within the 95% confidence limit when a few percent of the cells is misclassified due to missing or spurious extra spots. This misclassification can be caused by several underlying conditions, such as an imperfect hybridization efficiency, colocalization of the in situ spots [either due to projecting the three-dimensional cell into a two-dimensional microscopic object or to somatic pairing (3,16)], or the missing of spots that are out of focus or the misinterpretation of split spots. In cases when a high number of cells have to be analyzed, automation may be of help to process the slides more efficiently.

This paper describes a system for the automated counting of ISH results using brightfield microscopy. Both the hardware system aspects and the software image analysis algorithms for nuclei and spot detection are addressed. Screening a slide or a part thereof results in a frequency spot distribution of the interphase cells found. Additionally, the system offers several facilities for interactive classification of the slides. The performance of the system was analyzed using a model system for trisomy consisting of a mixture of male and female lymphocytes hybridized with probes for chromosomes 7 and Y.

MATERIALS AND METHODS
Slide Preparation

Peripheral blood was obtained from one female and one male, both healthy persons. The mononuclear fraction was separated by Ficoll gradient centrifugation (1.077 g/cm^3, 200g, 20 min, 20°C). The concentration of the cells was determined using a Sysmex microcell counter-F800. The results of three measurements were averaged and samples containing the different ratios of female and male cells were made. After heat denaturation, the preparations were hybridized with the following chromosome specific probes: alphoid DNA of chromosome 7 (24) and satellite DNA in the pericentromeric region of chromosome Y (ATCC DYZ3). Preparations of slides, predigestion steps, probe labeling, hybridization, posthybridization washings, and immunodetection of the hybridization signals were optimized for automated analysis. The hybridization result was visualized with peroxidase-diaminobenzidine (DAB) using hematoxylin as the DNA counterstain. Detailed protocols are described more extensively elsewhere (20).

System Description

The system is composed of an automated microscope and a Macintosh IIfx computer, which performs image processing and controls the functioning of the microscope. The microscope is an Ergolux (Leica, Germany), which is equipped with a scanning stage (Märzhäuser, Germany), a focus motor drive (Leica), a computer controlled objective rotor (5 positions), and an automated filter wheel (5 positions). The filter wheel is placed in front of the halogen lamp for wavelength selection in brightfield applications. A ×25 Plan Apo objective (NA 0.7) resulting in a field size of 254 × 178 μm was used for spot counting in combination with a Schott bandpass PAL 466 nm interference filter (with a bandwidth of 20 nm). The scanning stage is equipped with 2 mm spindles and is driven by a MAC-4000 stepping motor controller (Märzhäuser). The maximum stepping frequency is 40 kHz, which corresponds to a maximum speed of approximately 10 cm/s. This speed is only reached during relocation. As stage movement is accelerated and slowed down, the actual time to move from field to field including stage settling time is approximately 250 ms. The focus motor and filter wheel are controlled by the same stepping motor controllers, which have been interfaced to the two standard serial interfaces of the Macintosh. A LAB-NB board (National Instruments, Baltimore, MD) regulates the halogen lamp by means of a 12 bit DA converter and controls the objective rotor by means of five parallel IO lines. As an image sensor, a Sony CCD camera, XC-77RR-CE, is used. This video camera has 756 × 581 squared pixels of 11 × 11 μm and has capabilities for on-chip integration. Although the chip is not cooled, the dark current is internally compensated resulting in a good linearity and signal to noise ratio for integration times up to 15 s, which is sufficient for most fluorescence in situ hybridization (FISH) specimens (23). The images are captured by a frame grabber (Data Translation, Marlboro, MA) with a resolution of 768 × 512 pixels. The Macintosh IIfx is furthermore equipped with 32 Mb memory, a 160 Mb disc, and a 19 in. RasterOps color display provided with an accelerator board, which displays images of 1,024 × 768 pixels in 24 bit color.

Since the system is not equipped with hardware dedicated for autofocusing, the optimal focus position is found by analyzing images taken at different focus levels with the Macintosh processor itself. As focus criterion the squared gradient, summed over the entire image, is opti-

mized. This criterion was suggested as one of the best methods in some comparative studies (9,10). In order to reduce the analysis time the focus function is only based on 10% of the pixels equally distributed over the image. The squared gradient for those pixels is, however, calculated on their directly neighboring pixels. Slides are screened using a meander pattern. It was found sufficient to focus once every third field in the X- and Y-directions of the stage and to follow the trends of the variation in the Z-direction by calculating the optimal focus position for the fields in between by means of a bilinear predictive interpolation scheme, so that both of the trends in the X- and Y-directions are taken into account. When empty fields are encountered, autofocusing is postponed until the next field. However, as the cell density was controlled using centrifugation buckets (20), empty fields did not form any problem for this study.

Detection of Interphase Nuclei and In Situ Spots

The counting of spots in interphase nuclei involves two segmentation steps: first the detection of the nuclei and then the individual spots. In order to process images efficiently using a personal computer, data reduction is necessary at an early stage of the analysis. Therefore, the locations of the candidate nuclei are first roughly determined in order to reduce a complete image to regions of interest. A more accurate segmentation algorithm is subsequently applied only within these regions in order to define the contours of the objects more precisely.

The preprocessing step is performed in the following way: the images are subdivided into boxes of $n \times n$ pixels ($n = 16$ for the magnification used) and the integrated density per box is determined by summing the densities of the individual pixels within a box. When a box exceeds a predefined threshold, it becomes selected according to the following formula:

$$\text{Density}_{box} = \sum_{x \in box} \sum_{y \in box} (I_0 - I(x,y)) > T_0$$

where $I(x,y)$ = the grey value of the pixel at position (x,y); I_0 = the background value, i.e., the intensity value of the peak of the histogram of the whole image; and T_0 = a user-defined threshold.

When a cluster of more than five connective boxes is found, it is expanded in all directions with half of the box size. The smallest circumscribed rectangle of the newly formed cluster then becomes a region of interest (ROI). The parameter settings were adjusted in such a way that the ROIs included the entire nucleus plus sufficient background.

The more accurate segmentation of the nuclei is based on a combination of thresholding and edge detection and is performed at full resolution within each ROI separately. The threshold level D_0 is calculated as the grey value, where the distance between the grey-value histogram and a hypothetical line going through the background peak and the origin of the histogram is maximal (26). This global threshold appears to be too high (too close to the background peak) for correct segmentation of the nuclear boundaries throughout the whole image and would also select small parts of the background in the corners of the

image due to shading. As other global threshold settings were also insufficient to obtain a correct segmentation, the threshold D_0 is combined with edge detection based on the slope of the intensities in the horizontal direction. When the intensity of a pixel $A(i,j)$ is below the threshold D_0 and has a gradient higher than a preset constant C_0,

$$A(i,j) < D_0 \cap (A(i - 1,j) - A(i,j)) > C_0$$

and the pixel $A(i,j)$ becomes an object pixel. The next pixels along the line become also object pixels until a similarly steep backward slope is detected or when the intensity exceeds threshold D_0. Finally, a number of erosions are carried out followed by a filling operation in order to remove small artifacts such as cell fragments or pieces of dirt. Parameters, such as box size, cluster size, threshold T_0, constant C_0, and the number of erosions used, are dependent on magnification, cell type, and quality of the slides. These parameters can be tuned by the operator on a trial and error base. Windows are provided to show directly the effect of changing parameter settings to facilitate this process. The quality of the slides used in this study was such that all slides could be processed using the same parameter settings. Alternative segmentation methods, such as subtraction of a background image composed from merged empty fields or min/max filtering to compensate for image shading, have not been investigated, although this may improve the robustness of the segmentation procedure.

Following nucleus selection the spots within the cells are initially segmented based on the contrast differences between the spots and the counterstain. The actual detection relies on the following equation:

$$B(x,y) = 1 \text{ if } D_x(x,y) > T_1 \text{ or } D_y(x,y) > T_1$$
$$B(x,y) = 0 \text{ otherwise}$$

where $B(x,y)$ = the pixel (x,y) of the resulting binary image containing the spots; $D_x(x,y) = \text{MIN}(A(x + d,y), A(x -d,y)) - A(x,y)$; $D_y(x,y) = \text{MIN}(A(x,y + d), A(x,y - d)) - A(x,y)$; d = the distance corresponding to the expected width of the spots; $A(x,y)$ = the original grey value of the pixel at position (x,y); and T_1 = the predefined threshold depending on the contrast of the spots vs. the counterstain.

The threshold level T_1 is calculated as the difference between the average nucleus intensity and an estimate for the average spot intensity. On the basis of the grey-value histogram within the nucleus the average nucleus intensity is determined by averaging the intensities beneath the peak of this histogram. All intensities on the left side of the peak, i.e., intensities more than twice the standard deviation away from the peak, contribute to the calculation of the average spot intensity. As value T_1 is determined for each nucleus individually, the selection of spots becomes less dependent on variation in the counterstain due to differences in compactness between the cells. The initially segmented spots are expanded with a dilation cycle to prevent single spots from being fragmented. As a consequence, however, separate spots lying close to each other may also be merged together. Therefore, a watershed algorithm is carried out within the mask of each spot to see if spots will fall apart. Spots are only then separated when the area of the different parts and
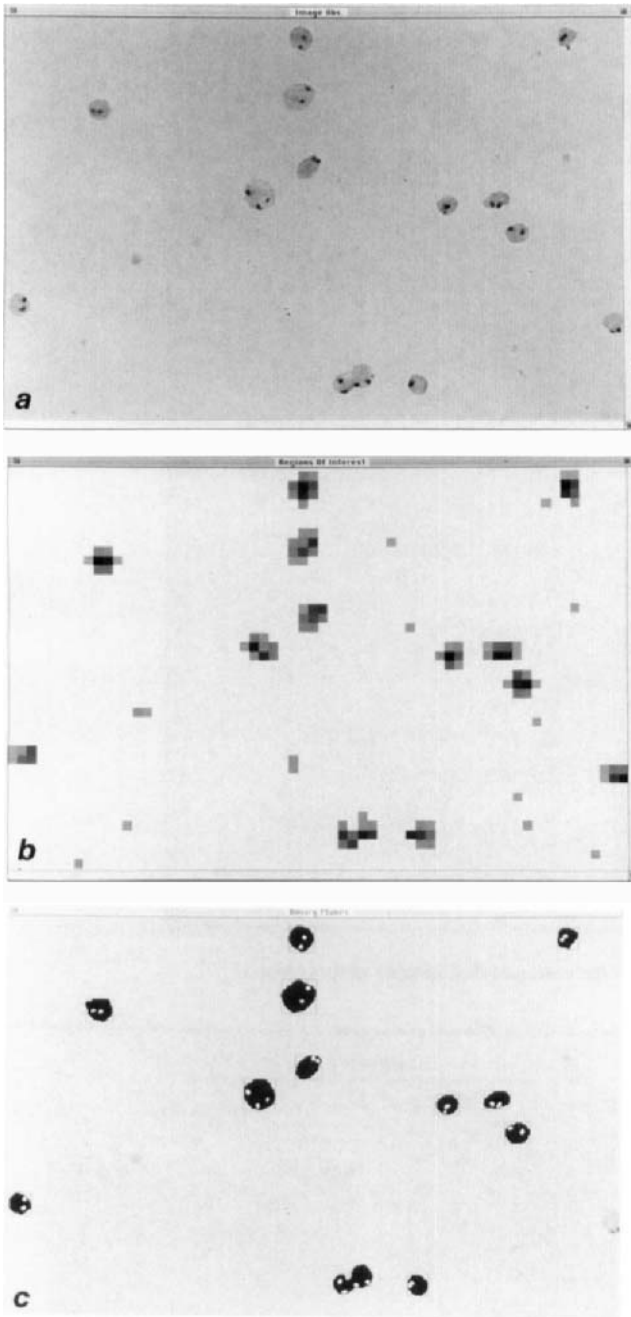
FIG. 1. a: Digitized image of a microscopic field containing blood lymphocytes labeled with a probe for chromosomes 7 and Y. b: The selection of ROIs. Boxes above threshold are shown in grey. Clusters of boxes will become ROIs. c: The result of the final segmentation. The selected cells (in black) and the spots found (in white) are indicated by a circumscribing rectangle. Touching objects have been discarded because of their size and shape, while objects touching the borders have been removed.

the contrast differences between the watershed separation line and the newly formed spots are large enough. The segmentation of interphase nuclei and the ISH spots are illustrated in Figure 1.

Feature Extraction and Cell Selection

Following nuclei and spot detection, a number of features are calculated for each candidate nucleus. These are the area of the nucleus, its contour length, the contour ratio (4π.area/contour^2), the integrated density, and the grey-value distribution of the nucleus in 16 classes. The latter distribution was determined by rescaling the histogram down to 16 equidistant classes and normalizing them on the area of the nucleus. The contribution of the spot signals was, however, not excluded when these features were calculated. The features can be applied for cell selection. The contour ratio and the area of the nucleus were found to be the most discriminative features for the model study based on blood lymphocytes. The discriminative power of the features was evaluated using the Fisher ratio on a learning set of a few hundred cells and artifacts (overlapping cells, pieces of dirt). In this study objects with a contour ratio of less than 0.8 were rejected under the assumption that it is less important that eventually some single cells are missed, as long as enough cells are being detected. It is also assumed that the roundness of a nucleus is not related to the chromosomal aberration itself and has no significant influence on the diagnosis. Obviously, the selection criteria can be adapted depending on the type of specimens analyzed.

For each potential spot, the total density, the peak density, and the area are calculated in order to decide whether a candidate spot is a "true" spot or not.

User Interface

The program for the automated spot counter is embedded in a user interface written according to Macintosh conventions resulting in a user-friendly environment. Dialogue boxes are provided to control the automated microscope, to adjust parameters for tuning the algorithm, to define the features for cell and spot selection, and to specify the scan area of the slide and/or the maximum number of cells that have to be analyzed. Windows are available during screening to show the performance of the image analysis algorithms and the data of the cells analyzed. As a result of the automated analysis, the system provides the frequency spot distribution together with the slide position and the measured feature values of each individual cell. Also the image of each cell found is stored in a gallery, as is shown in Figure 2. The operator can scroll through this window or rank the cells according to the number of spots found. This allows the operator to select quickly only the nuclei classified as being abnormal for visual inspection. When relocating the cells, the operator can overrule the automated classification by visually scoring the number of spots. During this interactive analysis the frequency spot distribution is corrected, while a confusion matrix between visual and automatic scoring is also built up. This is illustrated in Figure 3.

Model Study

In order to analyze the performance of the automated spot counter a model study was carried out with artificial mixtures of male and female cells in various proportions. As a model for trisomy, a cocktail of centromeric probes for chromosomes 7 and Y was used. The male and female cells were mixed in the following proportions: 1:99, 3:97, 5:95, 10:90, 40:60 [listed as (7+Y):7]. To generate the spot distribution, 1,000 nuclei per slide were analyzed.

The multiple proportion test is often used to examine whether the obtained spot distribution is abnormal or not
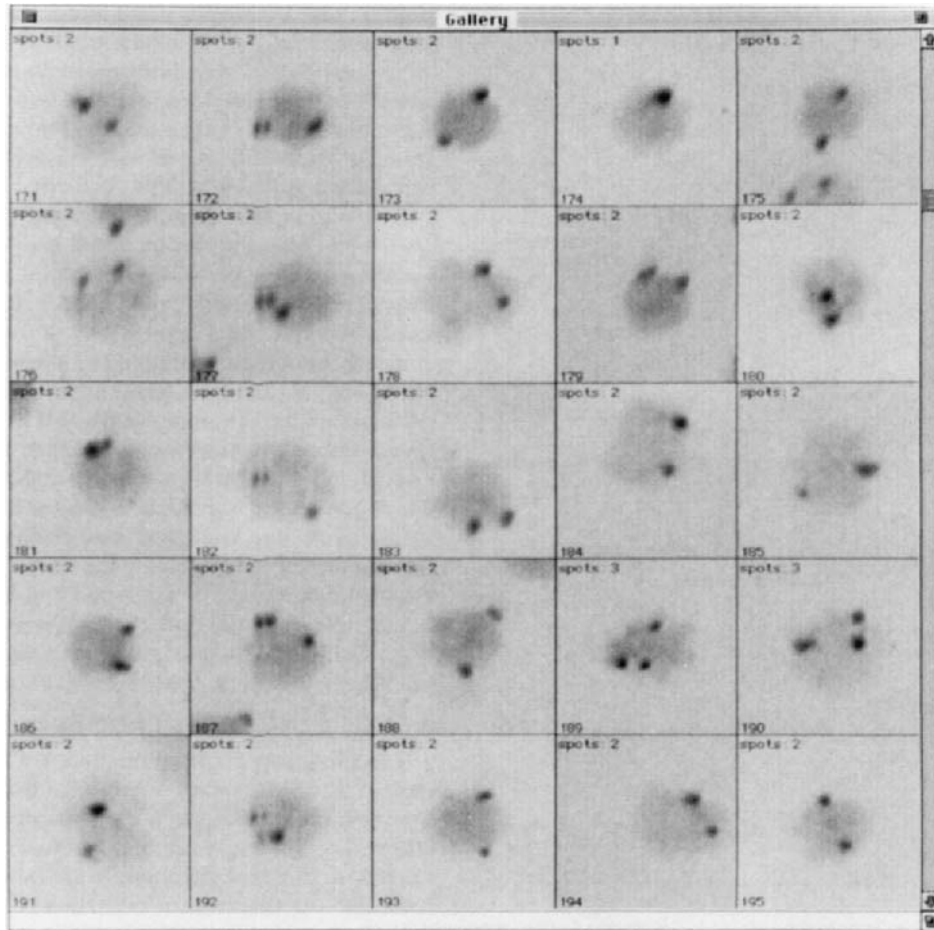
FIG. 2. A gallery window with selected cells and the corresponding number of spots found.
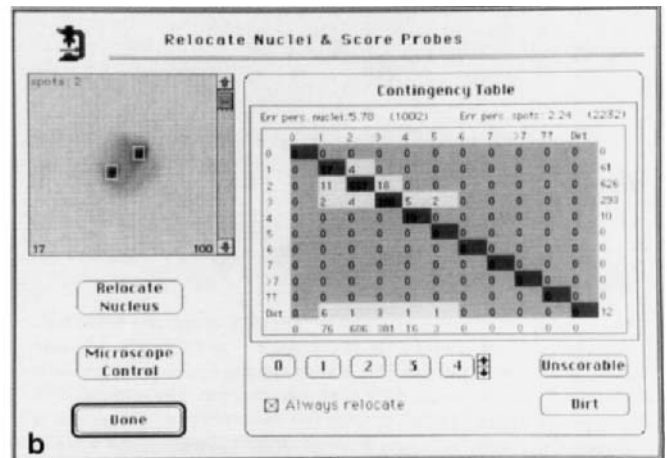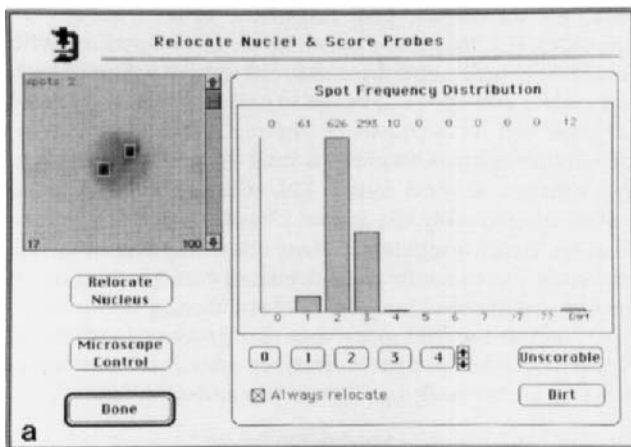

FIG. 3. a: The user dialogue for scoring cells interactively showing the current spot distribution. b: The user dialogue for scoring cells interactively showing the contingency table.

(1,2,12,14). In this test it is evaluated whether the observed proportion of cells with k-spots (k = 0,1,2,3) in the distribution of the test slide is higher or lower than the mean plus or minus twice the standard deviation for the corresponding proportion in the distribution of the control series. An abnormality is detected when at least one of the proportions is significantly different. Benchmark

results were obtained by Kibbelaar et al. (14) using this test for a similar study on manually classified specimens.

In this study we investigated what percentage of trisomic cells could still be detected as being abnormal under the following conditions: 1) the analysis was carried out completely automatically; 2) only those cells were reviewed which were found by the machine to have

three spots or more; 3) all cells analyzed by the system were visually evaluated. In order to determine the normal background frequency of trisomic nuclei, slides with 100% female cells were prepared and analyzed.

RESULTS

The results of the seeding experiment of male and female lymphocytes labeled with a probe for chromosomes 7 and Y are presented in Table 1. It shows the spot distribution for the various dilutions both after automatic classification and after reviewing all the cells by the operator. The operator was blind for the actual true mixed proportion of cells during this reviewing process. The automated classification may be corrected either on the basis of the digital cell image stored in the gallery, the analogue image of the relocated cell on the TV monitor, or by looking directly through the binoculars of the microscope. Although looking through the eyepieces provides the opportunity to focus up and down for checking the number of hybridization spots, the depth of focus on the ×25 objective is such that most cells could be directly classified correctly on the basis of the digital cell image or the analogue image on the TV monitor. Furthermore, Table 1 shows the percentage of trisomic cells after reviewing only those cells which were classified by the system to have three spots or more. During screening the cell selection criteria were adjusted in such a way that cells without spots were rejected by the system as it appeared that most of those cells were out of focus upon digitization. It was assumed that this would not influence trisomic spot detection. The corresponding column for the proportion of cells with zero spots is therefore missing in Table 1.

In order to determine the background frequency of trisomic cells labeled with the probe for chromosome 7, four spot counting measurements were performed on different parts of two control slides containing blood lymphocytes of females cells only. The results of the corresponding automatic and interactive spot distributions are shown in Table 2. The mean proportions, the standard deviations thereof, and the mean proportions plus and minus twice the standard deviation, as limits for the multiple proportion test, are also given. In view of the seeding experiment it means that all cases with a frequency of trisomic cells of 3% and higher were picked up as being abnormal on the basis of the multiple proportion test. This applies both for the automatic classification, the one after reviewing only the cells classified by the system to have three spots or more, and the one after reviewing all the cells by the operator. In the case of a frequency of 1.5% trisomic cells, the trisomic proportions for the automatic and interactive analysis were higher than the control, although not significantly. However, the monosomic proportion of the cells after interaction differed significantly from the control. In the case of a frequency of 0.8 trisomic cells, no significant differences were found on the basis of the multiple proportion test.

The total analysis time to select and count 1,000 cells per slide was 10 min and 45 s on average, from which 3 min and 55 s was necessary for autofocusing. One slide, i.e., sample 6, was not taken into account, as its performance differed considerably. The analysis time for that slide was 42 min and 15 s, from which 16 min and 46 s was

devoted to autofocusing. It appeared that its cell density was very low, i.e., 0.8 cells per microscopic field, so that 1,200 fields had to be analyzed in order to count the spots of 1,000 cells. The average cell density for the other slides was approximately 4 cells per microscopic field. The additional time necessary for evaluating 1,000 cells visually varied from 5 to 10 min depending on the number of cells which had to be evaluated though the binoculars of the microscope; relocating the cells and displaying them in the middle of the screen were carried out instantaneously. When the approach was chosen to evaluate only the cells which were classified to have three spots or more, the time necessary for interaction decreased significantly as only a fraction of the cells had to be reviewed.

The contingency tables between the automatic and visual analysis for the cells analyzed in the seeding experiment and the control slides are shown in Tables 3 and 4, respectively. The row "Artifact" in these tables shows the number of dirt particles and overlapping or broken cells which were selected and analyzed by the system as being single cells. For the seeding experiment this percentage was very low, i.e., 0.37%. Thus, in the case of blood lymphocytes, shape and size appear to be sufficient parameters for single cell selection. The percentage of false negative cells, i.e., the percentage of single cells rejected by the system, was not really investigated assuming that it would not bias the classification results. Visual observation during screening, however, indicated that almost all single cells were selected by the system. According to Table 3, 93.3% of all cells analyzed in the seeding experiment were classified correctly. In case of partial interaction, i.e., visual evaluation of only those cells which have three spots or more, 6.2% of the trisomic cells were missed, while the false positive rate was 18.8%. Similar results were obtained for the control slides (Table 4). Single cell selection was incorrect in 0.35% of the cases, while 97.2% of all single cells were correctly classified. In case of reviewing only the cells having three spots or more, 19.2% of the trisomic cells were missed, while the false positive rate was 22.2%. Causes for missing spots were that spots were too dim to be selected, that the cells were analyzed slightly out of focus, or that the spots were located too close to each other to be separated by the spot splitting algorithm. The detection of extra spots was mostly caused by small chromatin clumps in the counterstain or by small pieces of dirt laying on top of the cells.

DISCUSSION

The use of ISH for the study of numerical aberrations has a number of advantages compared to conventional cytogenetics. It can be applied both in metaphase spreads and in interphase cells, while the sensitivity of ISH for detecting numerical aberrations can be considerably higher than with conventional cytogenetics. It is much easier and faster to analyze about 500–1,000 interphase cells (thereby improving the statistics) than evaluating 20–50 metaphases with conventional banding techniques. Therefore, the technique is especially suited for cases where it is difficult to prepare good quality chromosomes due to a low proliferation activity of the tissue or in case of heterogeneous cell populations, such as in tumors (7,12,17).

In this paper the development of a system has been

Table 1

Automatic and Interactive Spot Distributions for the Slides of the Seeding Experiment[a]

Sample	Probe (7+Y):7	Automatic scoring (N = 1,000)					After interaction (trisomic cells)	After interaction (all cells)			
		1	2	3	4	5	3	1	2	3	4
1	100	2.6	23.1	67.2	6.4	0.7	71.0	1.3	20.4	77.5	0.8
2	50	5.6	59.2	31.6	3.5	0.1	29.4	6.0	62.8	31.0	0.2
3	25	6.4	68.0	23.7	1.9	0.0	18.3	6.0	73.8	19.3	0.9
4	12	11.6	75.9	12.3	0.2	0.0	11.6	9.6	78.2	11.7	0.5
5	6	9.5	84.9	5.3	0.3	0.0	4.2	8.6	86.9	4.4	0.1
6	3	9.8	85.3	4.7	0.2	0.0	3.9	9.2	86.6	4.1	0.1
7	1.5	13.2	84.1	2.6	0.1	0.0	2.4	12.0	85.2	2.7	0.1
8	0.8	14.4	83.1	2.4	0.1	0.0	1.7	13.4	84.8	1.7	0.1

[a]The first two columns list the sample designations and their respective ratios of male (77Y) and female (77) cells. The percentages of cells with k-spots per cell (k = 1–5) as found by the machine are given in columns 3–7. The number of cells analyzed per slide was 1,000. Column 8 shows the percentage of trisomic cells after reviewing only the cells with three spots or more, while in columns 9–12 the percentages of cells with k-spots per cell (k = 1–4) are given after reviewing all of the cells.

Table 2

Automatic and Interactive Spot Distributions for the Measurements of the Control Slides[a]

Sample	Automatic scoring (N = 1,000)				After interaction (trisomic cells)	After interaction (all cells)			
	1	2	3	4	3	1	2	3	4
1	17.2	80.3	2.4	0.1	2.3	15.2	81.6	3.1	0.1
2	17.1	80.9	1.9	0.1	1.6	16.1	81.3	2.4	0.2
3	14.3	83.8	1.8	0.1	1.6	13.3	84.5	2.1	0.1
4	13.5	84.5	1.8	0.2	1.3	12.9	85.3	1.8	0.0
5	16.5	81.2	2.2	0.1	2.1	14.3	83.2	2.4	0.1
6	15.2	82.2	2.6	0.0	2.0	15.0	82.8	2.2	0.0
7	14.7	82.8	2.4	0.1	1.8	14.1	83.6	2.0	0.3
8	15.3	81.6	3.0	0.1	2.0	14.3	83.4	2.2	0.1
Mean	15.48	82.16	2.26	0.1	1.84	14.40	83.21	2.28	0.11
S.D.	1.35	1.46	0.42	0.05	0.33	1.03	1.34	0.39	0.10
Mean + 2 S.D.	18.18	85.08	3.1	0.2	2.5	16.46	85.89	3.06	0.31
Mean − 2 S.D.	12.78	79.24	1.42	0.0	1.18	12.34	80.53	1.5	0.0

[a]The first column lists the sample designations. The percentages of cells with k-spots per cell (k = 1–4) as found by the machine are given in columns 2–5. The number of cells analyzed per slide was 1,000. Column 6 shows the percentage of trisomic cells after reviewing only the cells with three spots or more, while in columns 7–10 the percentages of cells with k-spots per cell (k = 1–4) are given after reviewing all of the cells.

described for automated spot counting in interphase cells using brightfield microscopy. Such a system may be of help for analyzing large quantities of slides, in particular when the frequency of abnormal cells is low, as manual scoring is tedious and time consuming. The performance of the system was tested in a seeding experiment for trisomy. It was shown that trisomic proportions down to 3% could be detected both automatically and interactively, while the dilution of 1.5% trisomic cells could only be detected as being abnormal after reviewing all the cells. Only the proportion of monosomic cells was significantly different. This can be explained by the presence of the Y-signal in a number of cells which show one spot for chromosome 7, so that the monosomic proportion is lowered. This effect becomes more dominant for the mixtures with higher proportions of male cells, as can be seen in Table 1.

It was assumed that the sensitivity for trisomy detection would be increased by reviewing only those cells that were automatically found to have three spots or more. This approach would require little extra effort after automatic analysis. The false positive trisomic cells would be eliminated in this way, while the false negative rate, consisting of the cells which were automatically classified as being disomic or monosomic, would not be

influenced so that an underestimate of the true trisomic percentage is obtained. This is illustrated in Figure 4. The automatically determined trisomic proportion is almost always higher than that after visual classification of the cells which have three spots or more, as the percentage of false positive cells is included. (An exception is the case of 100% male cells where more trisomic cells were classified having four spots than the percentage of false positive cells.) The trisomic proportion after evaluation of all cells is again higher than that after partial interaction, as now the false negative cells are included. For this seeding experiment the approach of partial interaction, however, did not result in an increase of sensitivity when compared to completely automatic analysis.

Figure 4 also shows what the proportion of trisomic cells was after completely manual analysis of 200 cells per slide. The cells were also manually selected. A good correlation was obtained with the automatic and interactive analysis. For the cases with a high percentage of trisomic cells, however, a significantly higher percentage of trisomic cells was found in comparison to those derived from automatic cell selection. This would suggest that the operator is somewhat biased to select trisomic cells for evaluation. For the lower frequencies the completely

Table 3
Contingency Table Between the Automatic and Visual Analysis for All of the Cells Used in the Seeding Experiment[a]

| | Automatic | | | | | |
	1	2	3	4	5	Total
Manual						
1	621	37	1	0	0	659
2	94	5,506	164	11	0	5,775
3	5	89	1,329	94	5	1,522
4	0	0	0	23	5	28
Artifact	3	21	3	1	0	28
Total	723	5,653	1,497	129	10	8,012

[a]The columns show the number of cells with k-spots per cell (k = 1–5) as found by the machine. The rows show the number of cells with k-spots per cell (k = 1–4) based on visual classification. Broken, overlapping cells or pieces of dirt selected by the system are designated as artifacts. Along the diagonal the number of correctly classified cells is shown.

Table 4
Contingency Table Between the Automatic and Visual Analysis for All of the Cells of the Control Slides[a]

| | Automatic | | | | | |
	1	2	3	4	5	Total
Manual						
1	1,122	29	0	0	0	1,151
2	93	6,513	32	2	0	6,640
3	2	33	147	0	0	182
4	0	1	2	6	0	9
Artifact	23	7	0	0	0	30
Total	1,240	6,583	181	8	0	8,012

[a]The columns show the number of cells with k-spots per cell (k = 1–5) as found by the machine. The rows show the number of cells with k-spots per cell (k = 1–4) based on visual classification. Broken, overlapping cells or pieces of dirt selected by the system are designated as artifacts. Along the diagonal number of correctly classified cells is shown.

manual analysis resulted in a lower percentage of trisomic cells suggesting that the number of 200 cells is probably too low to detect such frequencies reliably. It should also be noted that the trisomic proportion of the sample with 100% male cells is only about 80%. This is partly due to the fact that two probes are used to create trisomy. If both give good results in 90–95% of the cells, the total efficiency becomes on the order of 81–87%.

This pilot study has shown that the sensitivity for detecting trisomy is sufficient. Monosomy detection, however, will be more difficult. It is known that the background frequency of monosomic cells is usually much higher (varying from 5 to 10% per chromosome) than that of trisomic cells due to the imperfectness of ISH and colocalization. On the basis of the control slides used in the seeding experiment the averaged background proportion of monosomic cells was 14.4%. This higher background value can be explained by the poorer localization of the spots inherent to enzymatic labeling. This will result in larger probe signals when compared to fluorescence labeling thereby increasing the chance for colocalisation and for diffusion of one of the signals. Also, the standard deviation of the monosomic cell proportion of the control was somewhat higher in comparison to the one of the trisomic cell proportion. This will hamper the detection of especially the lower frequencies of monosomic cells.
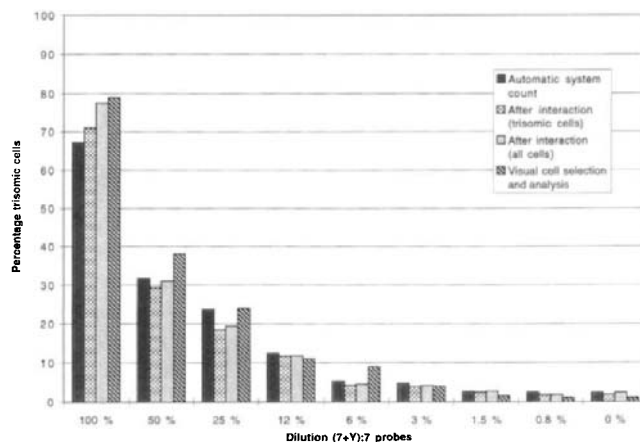

Fig. 4. The results of the seeding experiment of male and female lymphocytes labeled with a probe for chromosomes 7 and Y for trisomy detection.

A spot distribution based on control series is necessary in order to test whether the spot distribution of a test sample shows a significant difference or not. In the seeding experiment the reference distribution could be based on the same probes and the same cells (only 100% female cells) of the test samples. A percentage of 3% trisomic cells could be detected in this way. It should be mentioned, however, that the variability in the reference distribution between different individuals and between different batches of prepared samples has not been examined in this study. These factors may result in a decrease of the sensitivity for trisomy detection.

For clinical samples it is not always possible to determine the reference spot distribution based on the same cells and the same probes. Under such circumstances it may be useful to apply probes for other chromosomes on the same test samples or to apply the probes on samples of normal individuals. However, both methods can lead to inaccurate estimations for the reference spot distribution and thus to erroneous interpretations of the results. Results of other studies indicate that normal individuals may have a natural background level of monosomies and trisomies. To what extent these levels may vary between individuals and different chromosomes is currently unknown. These factors may, however, limit the sensitivity for trisomy or monosomy detection.

The software program is still not complete. Relatively simple parameters are being used for cell and spot detection. For the analysis of blood lymphocytes, as applied in the model study, the size of the nucleus and the contour ratio were sufficient to select single cells. It is likely that more sophisticated shape parameters or texture parameters may have to be analyzed to select reliably single nuclei in other cell types, e.g., for irregularly shaped bone marrow cells. Spot selection was only based on measurements of integrated density and area. It is desirable, however, to investigate whether other features, such as the mean and the variance of the density, are more discriminating.

Currently spots and nucleus are separated based on contrast differences, as a black and white camera is used for imaging. If images are digitized with a colorcamera, the additional color information could be applied to distin-

guish between spots and pieces of dirt and chromatin clumps, probably resulting in lower false positive and negative rates.

During the model study it became evident that the performance of the spot counting system depends to a great extent on slide preparation. There appears to be an almost linear relationship between cell density and the time necessary to analyze a slide. By applying centrifugation techniques it is possible to control the concentration of the cells. In the model study there were about four single cells (on average) per microscopic field of view. This resulted in an analysis time of somewhat more than 10 min to count 1,000 cells, from which one third of the time was required for autofocusing. Image processing was carried out on a Macintosh IIfx, which is a relatively old model. Running the spot counter algorithm on digitized images on a Power PC, model 8100/110, resulted in a speed increase of a factor 8 for image processing. However, the analysis time is not only dependent on processor power, but also on stage movement, the readout rate of the frame grabber, and the time necessary for focusing. Rough estimations suggest that the analysis time will drop to less than 5 min by upgrading the processor and by using a more efficient autofocusing algorithm based on interpolation instead of predictive extrapolation.

A spot counting system based on chromogenic labels using brightfield microscopy has clear advantages regarding speed of analysis. However, the sensitivity is limited and it is also difficult to increase the color multiplicity. When smaller target sequences or more than one probe has to be analyzed simultaneously, the use of fluorescence becomes a necessity. A similar system and program environment have been developed for fluorescence spot counting; encouraging results with this fluorescence system have been reported by Netten et al. (19).

ACKNOWLEDGMENTS

LITERATURE CITED

1. Anastasi J, Le Beau MM, Vardiman JW, Westbrook CA: Detection of numerical chromosomal abnormalities in neoplastic hematopoietic cells by in situ hybridization with a chromosome-specific probe. Am J Pathol 136:131–139, 1990.
2. Anastasi J, Le Beau MM, Vardiman JW, Fernald AA, Larson RA, Rowley JD: Detection of trisomy 12 in chronic lymphocytic leukemia by fluorescence in situ hybridization to interphase cells: A simple and sensitive method. Blood 79:1796–1801, 1992.
3. Arnoldus EPJ, Peters ACB, Bots GTAM, Raap AK, Van der Ploeg M: Somatic pairing of chromosome 1 centromeres in interphase nuclei of human cerebellum. Hum Genet 83:231–234, 1989.
4. Arnoldus EPJ, Wiegant J, Noordermeer IA, Wessels JW, Beverstock GC, Grosveld GC, Van der Ploeg M, Raap AK: Detection of the Philadelphia chromosome in interphase nuclei. Cytogenet Cell Genet 54:108–111, 1990.
5. Callen DF, Eyre HJ, Ringenbergs ML, Freemantle CJ, Woodroffe P, Haan EA: Chromosomal origin of small ring marker chromosomes in man: Characterization by molecular genetics. Am J Hum Genet 48: 769–782, 1991.
6. Carothers AD: Counting, measuring and mapping in FISH-labelled cells: Sample size considerations and implications for automation. Cytometry 16:298–304, 1994.

7. Van Dekken H, Pizzolo JG, Kelsen DP, Melamed MR: Targeted cytogenetic analysis of gastric tumors by in situ hybridization with a set of chromosome-specific DNA probes. Cancer 66:491–497, 1990.
8. Devilee P, Thierry RF, Kievits T, Kolluri R, Hopman AHN, Willard HF, Pearson PL, Cornelisse CJ: Detection of chromosome aneuploidy in interphase nuclei from human primary breast tumors using chromosome-specific repetitive DNA probes. Cancer Res 48:5825–5830, 1988.
9. Firestone L, Cook K, Culp K, Talsania N, Preston K: Comparison of autofocus methods for automated microscopy. Cytometry 12:195–206, 1991.
10. Groen FCA, Young IT, Ligthart G: A comparison of different focus functions for use in autofocus algorithms. Cytometry 6:81–91, 1985.
11. Hopman AHN, Poddighe PJ, Smeets AWGB, Moesker O, Beck JLM, Vooijs GR, Ramaekers FCS: Detection of numerical chromosome aberrations in bladder cancer by in situ hybridization. Am J Pathol 135:1105–1117, 1989.
12. Hopman AHN, Moesker O, Smeets AWGB, Pauwels RPE, Vooijs GP, Ramaekers FCS: Numerical chromosome 1, 7, 9, and 11 aberrations in bladder cancer detected by in situ hybridization. Cancer Res 51: 644–651, 1991.
13. Kibbelaar RE, Van Kamp H, Dreef EJ, Wessels JW, Beverstock GC, Raap AK, Fibbe WE, Den Ottelander GJ, Kluin PhM: Detection of trisomy 8 in hematological disorders by in situ hybridization. Cytogenet Cell Genet 56:132–136, 1991.
14. Kibbelaar RE, Kok F, Dreef EJ, Kleiverda JK, Cornelisse CJ, Raap AK, Kluin PhM: Statistical methods in interphase cytogenetics: An experimental approach. Cytometry 14:716–724, 1993.
15. Klinger KW, Landes G, Shook D, Harvey R, Lopez L, Locke P, Lerner TL: Rapid detection of chromosome aneuploidies in uncultured amniocytes by using fluorescence in situ hybridization (FISH). Am J Hum Genet 51:55–65, 1992.
16. Lewis JP, Tanke HJ, Raap AK, Beverstock GC: Kluin-Nelemans HC: Somatic pairing of centromeres and short arms of chromosome 15 in the hematopoietic and lymphoid system. Hum Genet 92:577–582, 1993.
17. Lichter P, Ward DC: Is non-isotopic in situ hybridization finally coming of age? Nature (London) 345:93–94, 1990.
18. Nederlof PM, Van der Flier S, Raap AK, Van der Ploeg M, Kornips F, Geraedts JPM: Detection of chromosome aberrations in interphase tumor nuclei by non-radioactive in situ hybridization. Cancer Genet Cytogenet 42:87–98, 1989.
19. Netten H, Young IT, Prins M, Van Vliet LJ, Tanke HJ, Vrolijk J, Sloos WCR: Automation of fluorescent dot counting in cell nuclei. In: Proceedings of the 12th IAPR International Conference on Pattern Recognition. Volume I, Conference A: Computer Vision and Image Processing (ICPR12, Jerusalem, Israel, October 9–13, 1994). IEEE Computer Society Press, Los Alamitos, CA, 1994, pp 84–87.
20. Van de Rijke FM, Vrolijk J, Sloos WCR, Tanke HJ, Raap AK: Sample preparation and in situ hybridization techniques for automated molecular cytogenetic analysis of white blood cells. Cytometry 24:156–162, 1996.
21. Suijkerbuijk RF, Mattopoulos D, Kearney L, Monard S, Dhut S, Cotter FE, Herbergs J, Van Kessel AG, Young BD: Fluorescent in situ identification of human marker chromosomes using flow sorting and Alu element-mediated PRC. Genomics 13:355–362, 1992.
22. Smit VTHBM, Wessels JW, Mollevanger P, Schrier PI, Raap AK, Beverstock GC, Cornelisse CJ: Combined GTG-banding and nonradioactive in situ hybridization improves characterization of complex karyotypes. Cytogenet Cell Genet 54:20–23, 1990.
23. Vrolijk J, Sloos WCR, Verwoerd NP, Tanke HJ: The applicability of a non-cooled video-rated CCD camera for the detection of fluorescence in situ hybridization signals. Cytometry 15:2–11, 1994.
24. Waye JS, England SB, Willard HF: Genomic organization of alpha satellite DNA on human chromosome 7: Evidence for two distinct alphoid domains on a single chromosome. Mol Cell Biol 7:349–356, 1987.
25. Ward BE, Gersen SL, Carelli MP, McGuire NM, Dackowski WR, Weinstein M, Sandlin C, Warren W, Klinger KW: Rapid prenatal diagnosis of chromosomal aneuploidies by fluorescence in situ hybridization: Clinical experience with 4,500 specimens. Am J Hum Genet 52: 854–865, 1993.
26. Zack GW, Rogers WE, Latt SA: Automatic measurement of sister chromatid exchange frequency. J Histochem Cytochem 25:741–753, 1977.